902322

Airbag Modelling Techniques

J.J. Nieboer, J. Wismans, and P.J.A. de Coo
TNO Road-Vehicles Research Institute
Delft, The Netherlands

ABSTRACT

This paper concerns the computer modelling of airbag restraint systems, particularly the aspect of contact interaction between the human body and the airbag. Two approaches can be distinguished for modelling the airbag. The earliest models use a non-deformable elliptical shape or a deformable shape based on line segments and circular arcs for representation of the airbag. Penetration volumes and contact forces are calculated in an empirical manner. A second approach uses the finite element method to simulate the bag material. The finite element bag can deform realistically and bag inertia forces are generated.

In this paper a comparison is made between simulation results obtained with the empirical airbag model in MADYMO 2D and the finite element airbag model in PISCES. Validation for both types of simulation has been carried out using impactor tests on sealed airbags. Parameters varied in these impactor tests include the impact velocity and the shape of the impactor face.

It will be shown that with regard to penetration of average and large sized objects both types of simulation provide reliable results. The predictions of the MADYMO 2D airbag model for relatively small penetrating objects are less adequate. This affects in particular passenger side airbag simulations.

Based on these findings it was decided to develop a three-dimensional airbag model in MADYMO 3D, using a finite element approach rather than an empirical approach as customary up to now in Crash Victim Simulation programs. The airbag in this model will be represented by 3-node membrane elements. A first demonstration of the MADYMO 3D airbag model will be given at the end of this paper.

THE USE OF COMPUTER SIMULATION TECHNIQUES in automotive crash safety design has rapidly increased in the past years. For the human body as well as for the car structure and protection devices, like seat belts and airbag, computer models are becoming more and more realistic. This paper concerns the computer modelling of airbag restraint systems, particularly with respect to the aspect of contact interaction between human body and airbag.

Since the early seventies several airbag models, simple ones and more sophisticated ones, have been developed. Most of these models were developed as an extension of an existing Crash Victim Simulation program, where the occupant is represented by a linkage system of rigid bodies. A survey of airbag models described in literature is given in Table 1. Among these empirical models the BDRACR, BPAC, MVMA-2D, MADYMO 2D and CAL-3D airbag models are best-known. In these models rather simple approximations for the contact interaction between human body and airbag are employed. The airbag is represented either by a non-deformable elliptical shape or a deformable shape based on line segments and circular arcs.

Recently finite element techniques have been applied for the simulation of airbag behaviour [9-11]*. With this approach the airbag deforms realistically when penetrated and generates bag inertia forces. Moreover, bag material properties can be incorporated in a direct way. If in addition an Euler discretization is used for the gas inside the airbag, gas blow forces can be simulated as well [12]. Disadvantages of the finite element approach, however, are the model complexity and the relatively long computer run times required. For practical use as in occupant

* Numbers in parentheses designate references at the end of the paper

protection studies it requires a coupling with a CVS program, since finite element programs do not provide features like various belt systems and realistic and efficient occupant models.

Table 1 Empirical airbag models

name	organisation	
VODS	Breed Corporation	[15]
DEPLOY	Fitzpatrick Engineering	[16]
BDRACR	Fitzpatrick Engineering	[1, 2]
BPAC	Fitzpatrick Engineering	[3]
MVMA-2D	HSRI (UMTRI)	[4, 5]
DJPAC	NHTSA	[17]
ABAG 19	Cornell Aeronautical Laboratory	[16, 18]
HSRI-3D	HSRI (UMTRI)	[18, 19]
CAL-3D	Calspan Corporation / GM	[7, 8, 17]
MADYMO 2D	TNO Road-Vehicles Research Institute	[6, 13]

The objective of this paper is to evaluate the empirical techniques for airbag modelling. For this purpose a comparison will be made between simulation results obtained with an empirical airbag model and a finite element airbag model. For the empirical model the MADYMO 2D airbag model was chosen. This model is considered to be representative for airbag models using a non-deformable bag shape to calculate penetration volumes and contact forces. The PISCES 2D-ELK code is used for performing the finite element simulations [12]. An important feature of this code is the coupling between the Lagrange/ shell discretization for the structural part of the model and the Euler discretization for the gasses. First impactor tests on sealed airbags were used to validate the finite element model. Due to the complexity of airbag interaction this study is focussed on axi-symmetric contact problems.

First the impactor tests on sealed airbags used for validation purposes are described in this paper. In these tests impactor shape, impact velocity and support of the airbag were varied. For simulation of these impactor tests with the PISCES 2D-ELK code the bag material properties are required. Therefor a series of uniaxial tensile tests were carried out on airbag material. The PISCES model set-up and validation results are presented. It is shown that this type of modelling results in a very detailed and accurate simulation of the airbag interaction. Using the validated model set-up the effect of a number of parameter variations is evaluated; these include variations of impact velocity, bag elasticity and bag support shape.

Subsequently, a number of finite element calculations is simulated using the MADYMO 2D airbag model. By comparing simulation results the empirical modelling approach is evaluated. Special attention is given to the effect of bag elasticity on the simulation results.

Based on the findings of this study it was decided to apply a finite element approach for developing a three-dimensional airbag model in MADYMO 3D. This model is optimized for airbag simulation in a CVS environment. A first demonstration of the MADYMO 3D airbag model will be presented. A discussion on major findings of this study and future developments in airbag modelling concludes this paper.

AIRBAG IMPACTOR TESTS

TEST SET-UP - The airbag used in this study is a generic driver side airbag. This bag has a volume of 60 liters and is neoprene coated. Figure 1 shows a lay-out of the flat bag. The bag has four exhaust orifices, each having a diameter of 35 mm. Extra airbag material and neoprene glue were used to close these orifices prior to testing. The pressurized bag geometry can be approximated by an ellipsoid having two semi-axes of 296 mm and one semi-axis of 163.5 mm. The total mass of the airbag is 405.8 grams, including the mass of six straps of about 290 mm in length each. These straps, located inside the bag, form a connection between back and front of the airbag, thus limiting the deployment range.

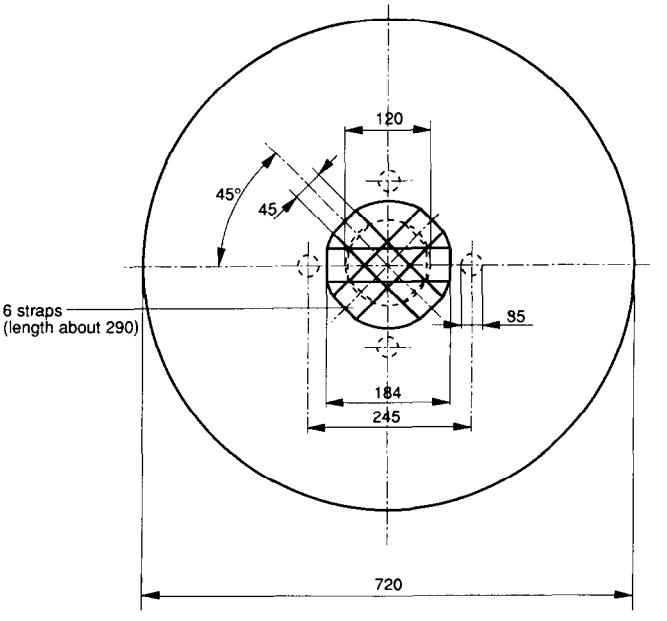

Fig. 1 Lay-out of the flat bag

Figure 2 shows the test set-up. The airbag is attached to a steel frame, which is mounted to a concrete block. The bag is supported either by a flat plate or a steering wheel. In order to eliminate steering wheel deformation, a steel rim and hub were used for representation of the steering wheel support. A pneumatic three-way valve and a needle valve can be used to fill or empty the airbag. The three-way valve is also used to isolate the bag volume from the supply system just before impact. Prior to each test the internal airbag overpressure was adjusted at 4000 N/m^2. The airbag is penetrated in the center by four different impactor faces at various impact velocities. Table 2 summarizes the relevant impactor data. Use was made of a guided spring-driven impactor configuration. During the test the impactor displacement, the impactor deceleration and the pressure inside the airbag were measured. The pressure transducer is fixed into the back of the steel support frame. The impact velocity was measured by means of two photosensitive cells installed at a known distance from each other. The maximum impact velocity is limited here, either by the spring stiffness or the guidance length, respectively in case a large impactor mass or a small impactor mass is involved. Table 3 summarizes the impactor test program.

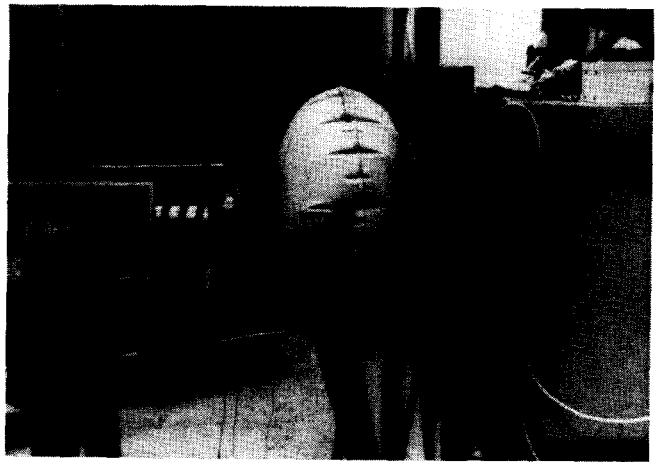

Fig. 2 Impactor test set-up

Table 2 Impactor description

shape	dimensions (mm)	total mass (kg)
half sphere	diameter 165	7.85
circular plate	diameter 80	5.98
circular plate	diameter 200	6.03
circular plate	diameter 500	8.05

TEST RESULTS ANALYSIS - After filtering of the signals at CFC 180, the airbag pressure versus impactor displacement and the impactor force versus impactor displacement were compared for different test conditions.

Table 3 Impactor test program

test no.	impactor	support	speed (m/s)
C96017	sphere 165 mm	flat plate	2.20
C96002 *	sphere 165 mm	flat plate	5.12
C96016	sphere 165 mm	flat plate	5.90
C96015 *	sphere 165 mm	steering wheel	4.80
C96009 *	circular plate 80 mm	flat plate	5.20
C96003 *	circular plate 200 mm	flat plate	3.90
C96022	circular plate 200 mm	flat plate	4.90
C96021	circular plate 200 mm	steering wheel	5.40
C96006 *	circular plate 500 mm	flat plate	4.70

* used for validation study

Figures 3 and 4 show the test results for different impactor faces and a flat plate support. In the force-displacement plot only the loading curves are included, because the unloading curves were disturbed by the rebound of the impactor face on the spring. Note that a transducer error is responsible for an initial negative force in test C96002. With different impactor faces and a steering wheel support, similar test results were obtained [14]. Compared with a flat plate support, a steering wheel support causes a slightly earlier increase in both airbag pressure and impactor force. In addition it was found that, except for a difference in penetration depth, the influence of impact velocity can be neglected for the considered test conditions. For increased penetration corresponding with higher impact velocities, however, this influence can become relevant.

SIMULATION OF IMPACTOR TESTS USING A FINITE ELEMENT PROGRAM

BAG MATERIAL PROPERTY TESTS - In order to carry out a finite element analysis, the mechanical properties of the airbag material have to be known. The airbag and straps consist of a two-thread nylon fabric. The bag is coated on the inside, while the straps are coated on both sides. Thicknesses of 0.5 mm and 0.6 mm were measured for the airbag and the straps, respectively. For the airbag material two series of two uniaxial tensile tests were carried out.

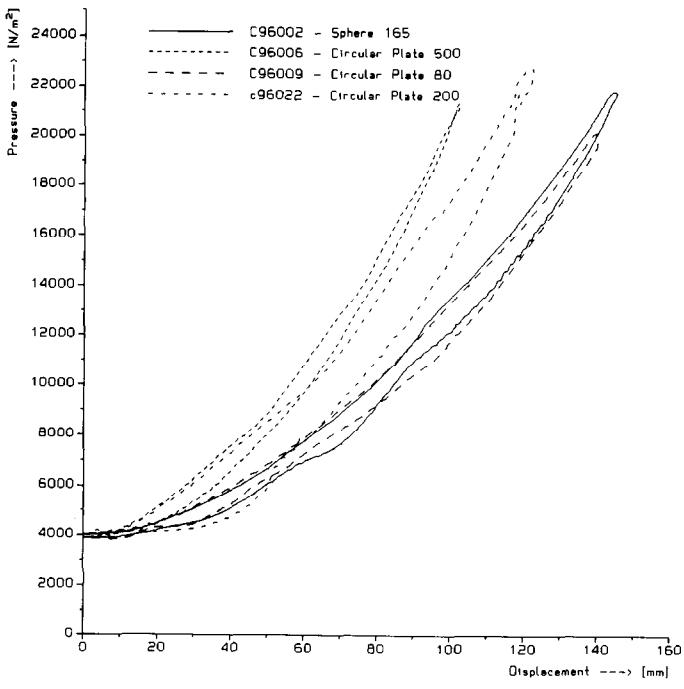

Fig. 3 Pressure versus displacement for different impactors and a flat plate support

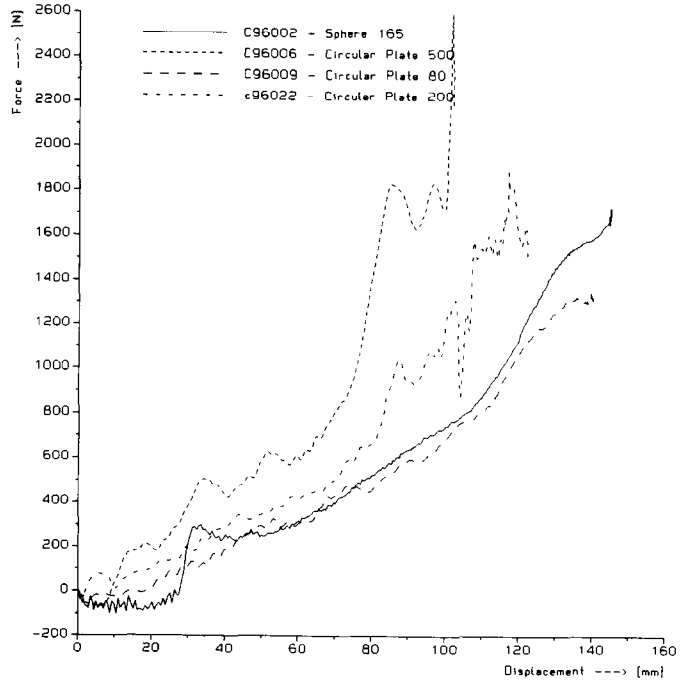

Fig. 4 Force versus displacement for different impactors and a flat plate support

One series using 32 mm wide specimen and another series using 50 mm wide specimen. Each specimen was tested in the warp and weft direction, these directions will be denoted here by the K- and I-direction. Figure 5 shows the test results for the airbag material. The K-direction proves to be stronger than the I-direction, due to a larger number of fibres or a tighter weave. The properties of the airbag material can be determined more accurately by pure biaxial tensile tests. For the strap material three identical uniaxial tests were carried out. The specimen here were actual straps, having a width of 45 mm. The weaving pattern has an angle of 45 degrees with respect to the length of the strap. Due to this weaving pattern a relatively soft behaviour can be observed. Figure 6 shows the test results for the strap material.

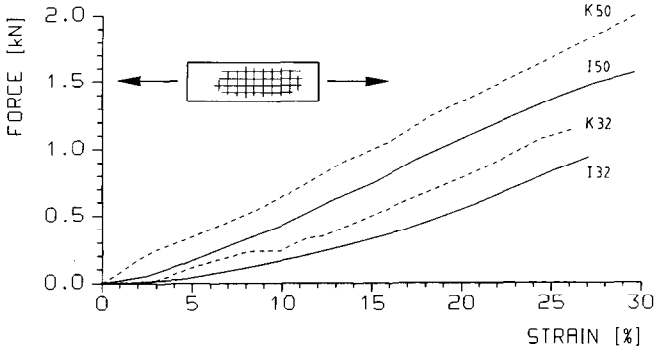

Fig. 5 Uniaxial tensile test results for 32 mm and 50 mm wide bag material specimen

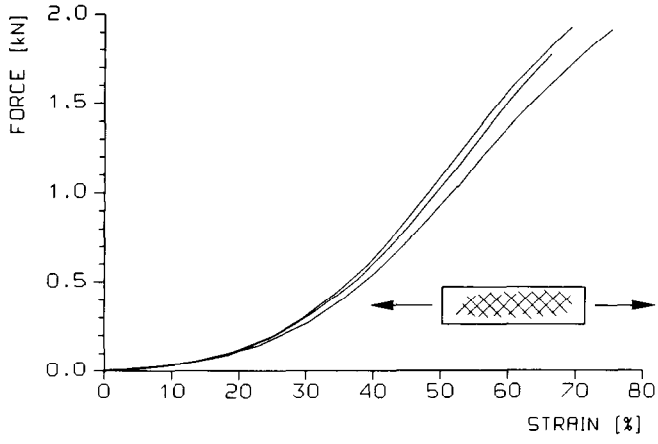

Fig. 6 Uniaxial tensile test results for the straps

FINITE ELEMENT MODEL SET-UP - The impact of a sealed airbag by a single rigid body will be simulated with the PISCES 2D-ELK code. The deployed airbag is assumed to be axi-symmetric, therefore an axial symmetric representation of the airbag is allow-

ed. The model consists of 24 axial symmetric shell elements. By using one integration point through the element thickness, only membrane forces are taken into account. The straps have been spread out circumferentially and are represented by a spring which constraints the displacement of a specific nodal point of the airbag. This spring has a fixed length and does not account for compression forces. At the front side of the airbag, where the straps are attached, a larger thickness for the bag elements is specified. Support and impactor face are modelled as rigid bodies. An asterisk (*) in Table 3 indicates the impact configurations simulated with the PISCES 2D-ELK code. The gas inside the airbag flows through an Euler grid. This grid contains 17x27 rectangular zones. A polygon along the nodal points encloses the gas inside the bag for defining the interaction between gas and bag. Contacts are specified between airbag and impactor face and between airbag and flat plate support or steering wheel support. Figures 7a and 7b show the initial model set-up when using a flat plate support and a steering wheel support respectively.

From the initial slope of the curves in Figure 5 an average Young's modulus for the bag material was derived, as only very low strain levels are involved here. The elasticity of the straps was calculated from the initial slope of the curves in Figure 6. Poisson's ratio is assumed to have a value between the values for steel and rubber. The material properties used as input for the finite element simulations are summarized in Table 4.

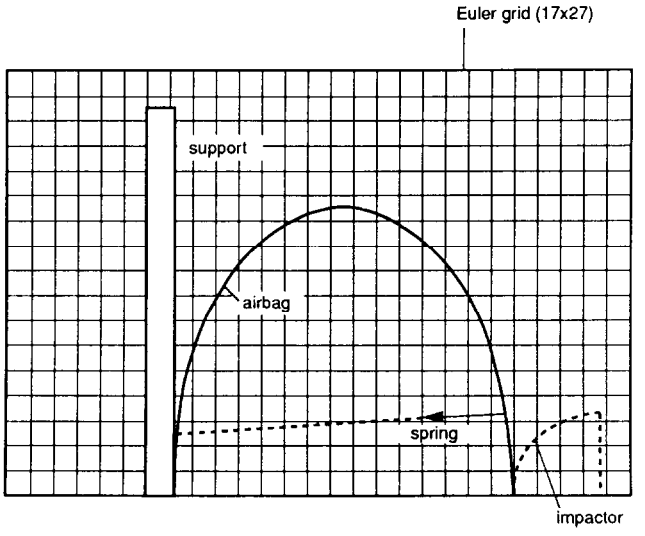

Fig. 7a Finite element model set-up with the flat plate support

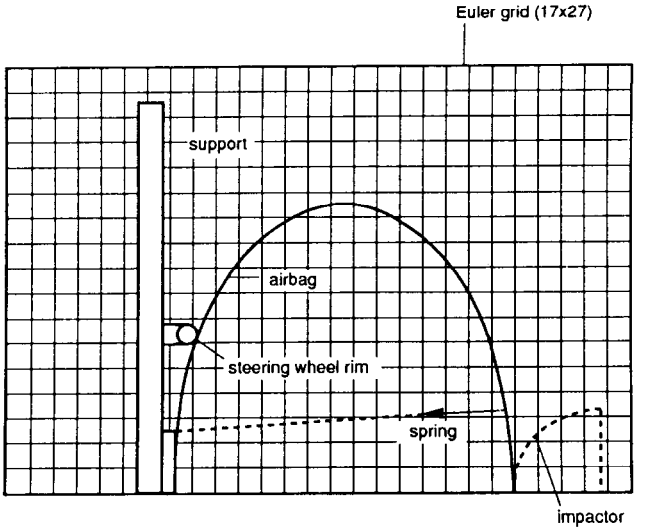

Fig. 7b Finite element model set-up with the steering wheel support

Table 4 Material properties

material	parameter	variable	units	value
airbag	thickness	t	mm	0.5
	density	ρ	kg/m^3	662
	Young's modulus	E	N/m^2	6.00E7
	Poisson's ratio	ν	-	0.4
straps	width	b	mm	45
	thickness	t	mm	0.6
	number	n	-	6
	Young's modulus	E	N/m^2	2.09E7
	initial length	l_0	mm	297
air	specific heat ratio	γ	-	1.4
	specific internal energy	e	J/kg	2.1388E5
	density	ρ	kg/m^3	1.2156
	const. vol. specific heat	c_v	J/kgK	730
	initial temperature	T_0	K	293
	initial overpressure	P_0	N/m^2	4000

SIMULATION RESULTS - Five impactor tests (see Table 3) have been simulated. The simulation results have been compared with the corresponding experimental results [14]. This comparison is presented for the sphere 165 mm impactor combined with either a flat plate support (Figure 8) or a steering wheel support (Figure 9) and the 200 mm circular plate impactor combined with a flat plate support (Figure 10). The comparisons for the circular plates having a diameter of 80 mm and 500 mm show a similar trend. Simula-

tion results for the probe displacement, probe acceleration and pressure change inside the airbag as a function of time are presented together with the experimental signals. A plot showing the airbag shape and the air velocity distribution after 40 ms is included as well. Note that the pressure is calculated inside the airbag near the inflator opening. In contrast to the experimental signal the calculated pressure is not filtered.

In general a good correlation between experiment and simulation can be observed. During the loading phase the displacement curves are almost identical. During unloading these curves slightly deviate due to the friction between impactor shaft and bearings in the actual test set-up. The simulated accelerations are almost a copy of the experimental ones. The oscillations in the unloading phase of the experimental curves are caused by the rebound of the impactor face on the spring of the impactor. The calculated pressure is about 15 % lower than the pressure measured in the experiments. This difference is probably caused by a systematic error in the pressure transducer, but a deviation in initial bag volume could be a contributory cause. From the correlation study it can be concluded that application of the finite element model results in a very reliable prediction of the test results.

PARAMETRIC STUDIES - The previous simulations and experiments show rather small impactor penetrations. In order to obtain larger penetrations and hence more airbag deformation, higher impact velocities have been applied. Higher strain levels are attainable when using higher impact velocities. A non-linear stress-strain curve, derived from Figure 5, will be used here. By varying the slope of this curve, the influence of weak and stiff bag material can be investigated (see Figure 11). Furthermore, simulations have been carried out with the support shape identical to the impactor shape and with small and large impactor faces. Table 5 summarizes the simulation program for the parametric study.

For easy reference not all simulation results are included here; a complete survey can be found in [14]. Figure 12 shows the "variation b" kinematics for the circular plate impactors combined with a flat plate support up to 10 ms. Figure 13 shows the relation between bag volume and impactor penetration (loading phase only) for the different circular plate impactors and different parameter variations. The corresponding contact force is given in Figure 14.

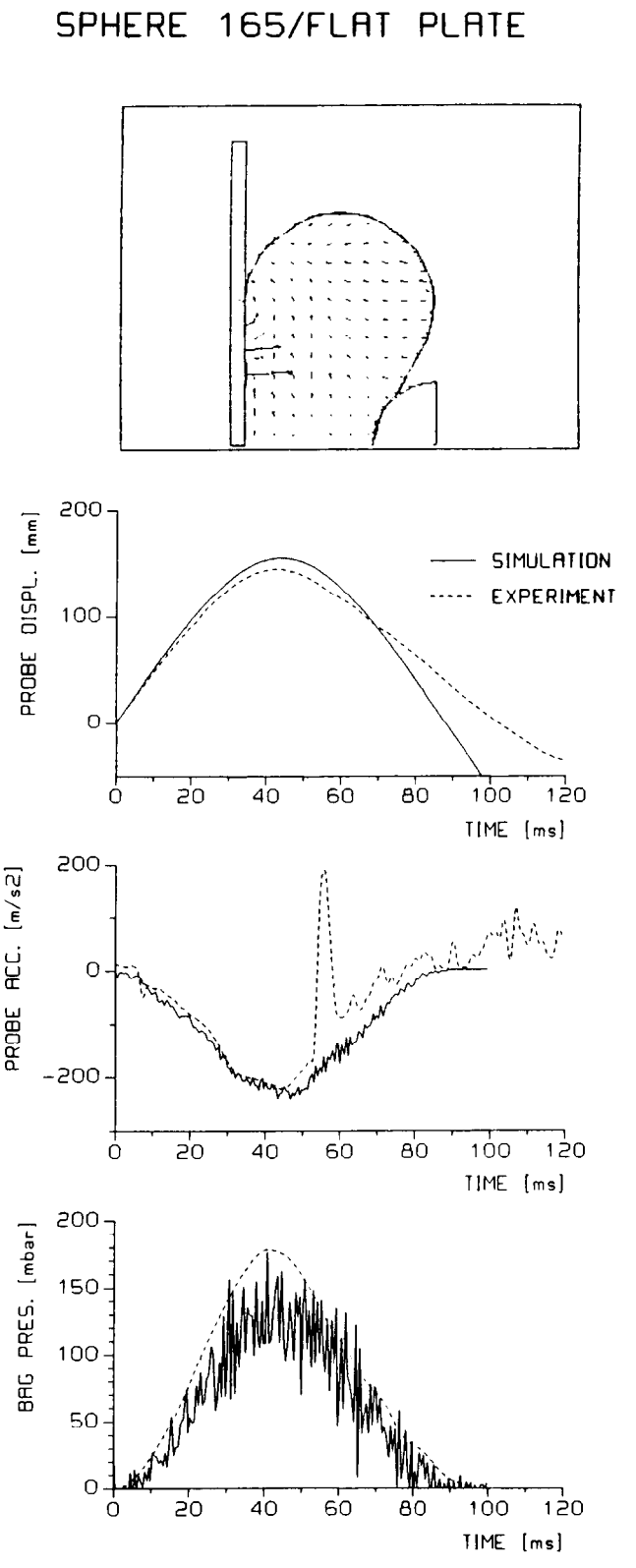

Fig. 8 Finite element model validation for the sphere 165 mm impactor combined with a flat plate support

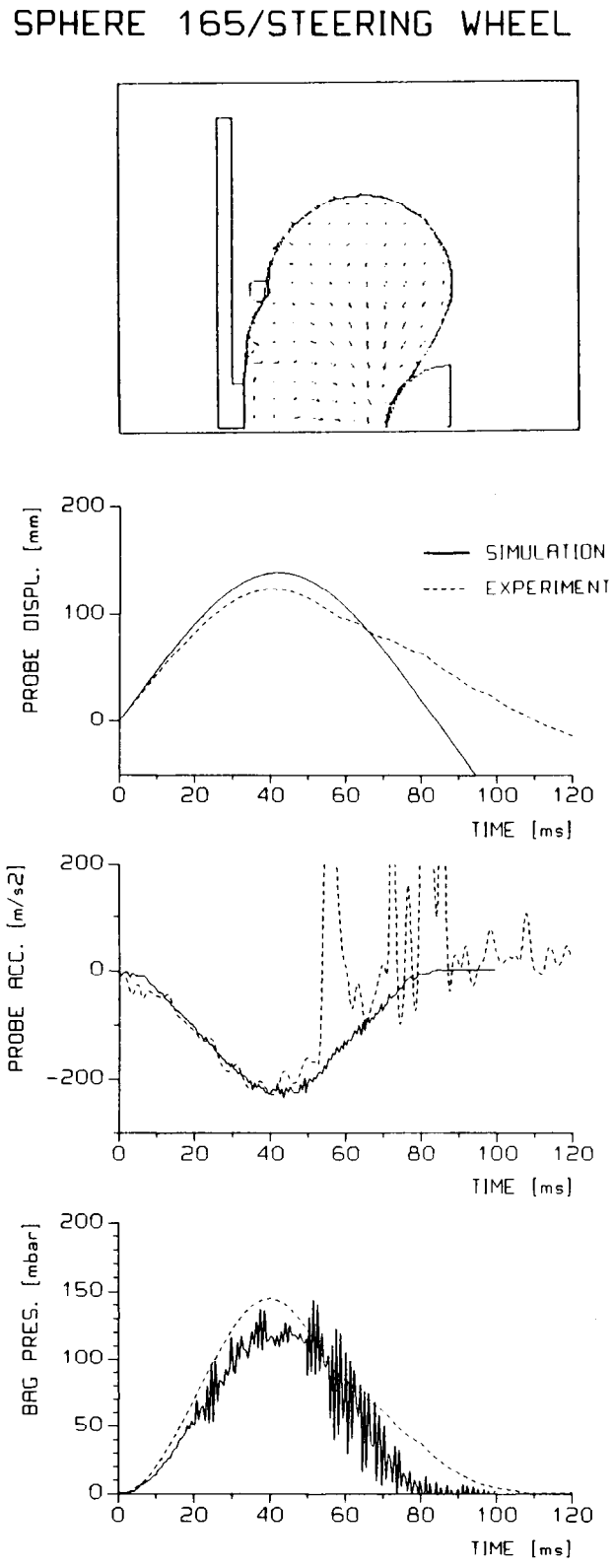

Fig. 9 Finite element model validation for the sphere 165 mm impactor combined with a steering wheel support

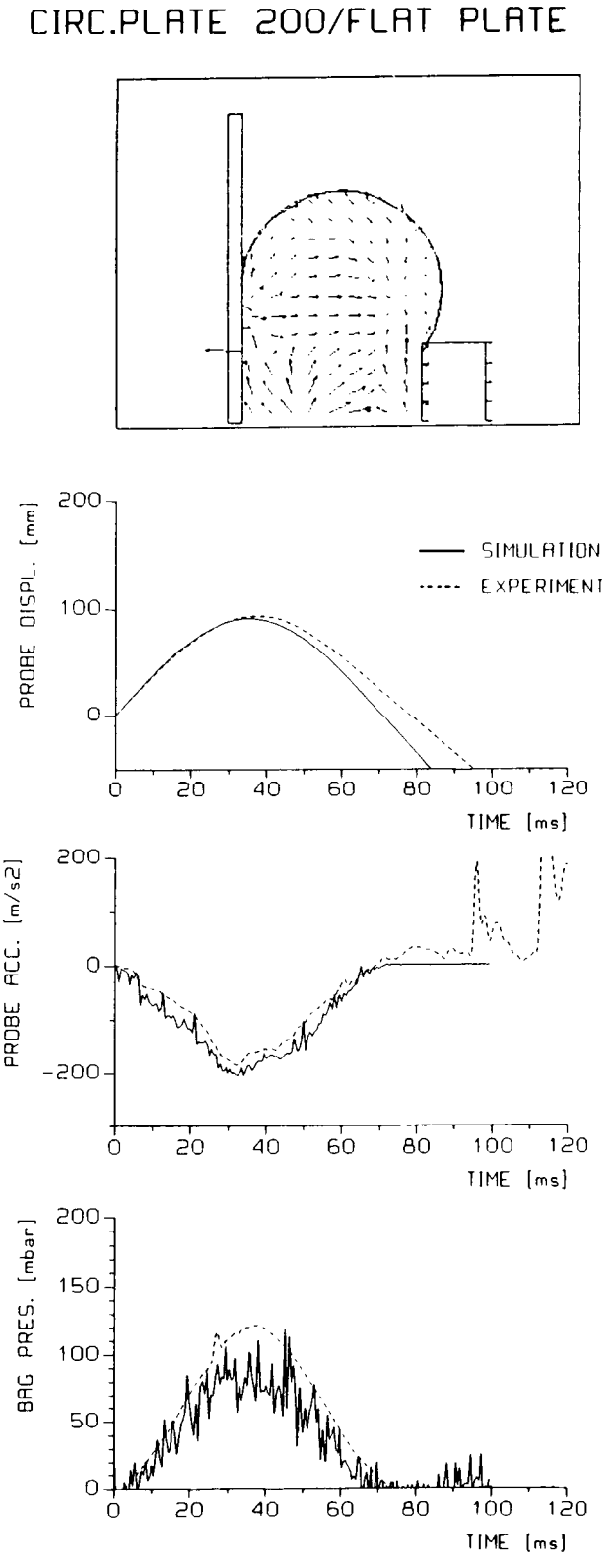

Fig. 10 Finite element model validation for the circular plate 200 mm impactor combined with a flat plate support

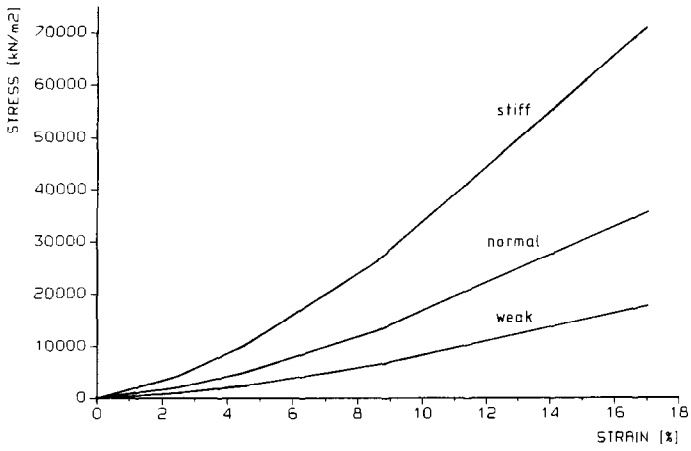

Fig. 11 Stress-strain curves for weak, normal and stiff bag material

Table 5 Simulation program for the parametric study

run	impactor shape	variation a norm. mat.	b norm. mat.	c weak mat.	d stiff mat.	e norm. mat./ impactor support
		impact velocity (m/s)				
1	sphere 165	5.12 *	10 *	10	10	
2	sphere 165/st. wheel	4.80	10	10	10	
3	sphere 500 **	5 *	20 *	20	20	
4	circ. plate 80	5.20 *	10 *	10	10	10
5	circ. plate 200	3.90 *	20 *	20	20	20
6	circ. plate 500	4.70 *	24 *	24	24	24
7	circ. plate 1000 **		24 *	24	24	

* also simulated with MADYMO

** mass 8.00 kg

It can be learned that for the finite element simulations the influence of impact velocity can be neglected (see Figure 14). This confirms the experimental findings. The bag elasticity directly affects the calculated bag volume. As expected a weak material causes a larger initial bag volume than a stiff material. Moreover, it was found that for larger impactor faces the individual bag volume and contact force curves tend to have the same shape during penetration.

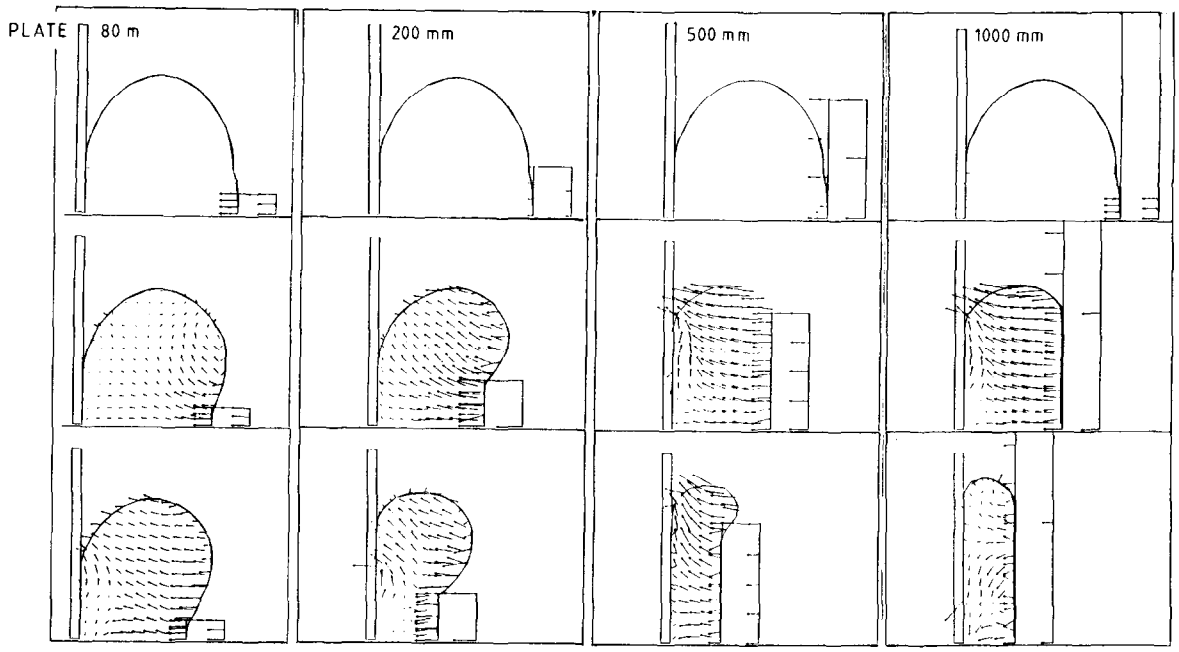

Fig. 12 Kinematics of the circular plate impactors for variation b up to 10 ms

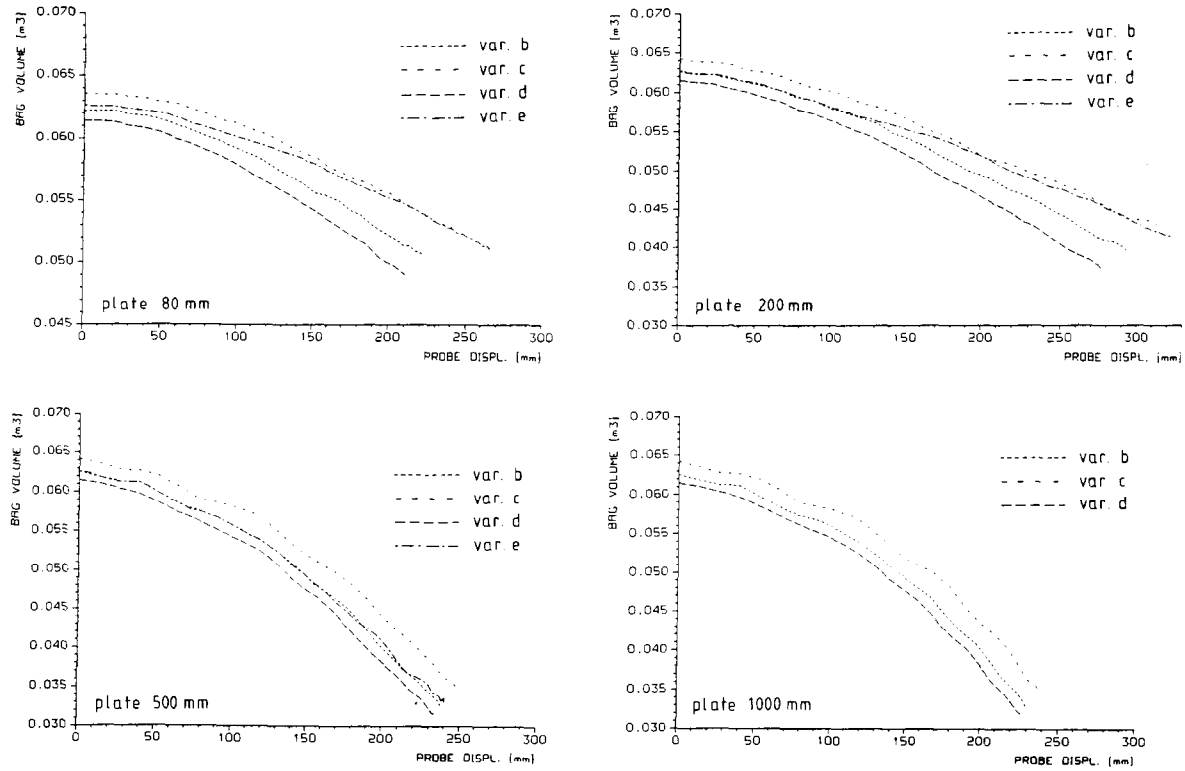

Fig. 13 Bag volume versus impactor penetration for different circular plate impactors and different parameter variations

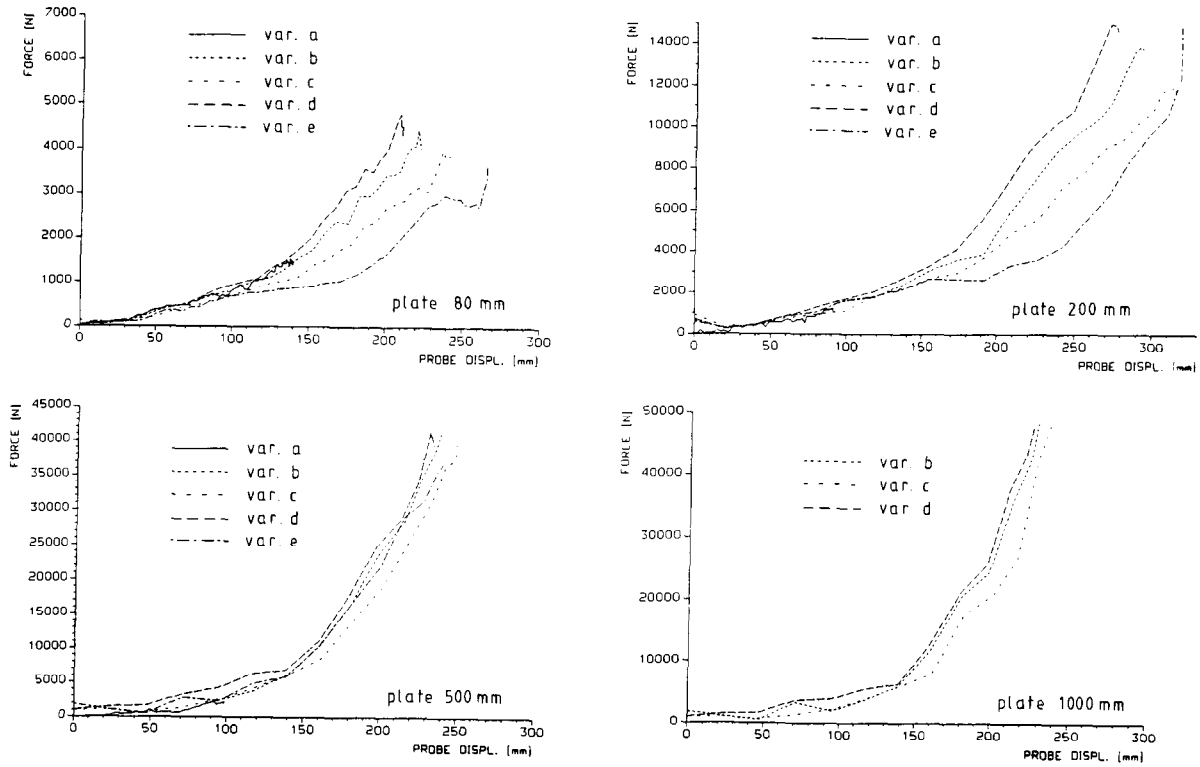

Fig. 14 Contact force versus impactor penetration for different circular plate impactors and different parameter variations

COMPARISON BETWEEN FINITE ELEMENT AND EMPIRICAL AIRBAG MODEL SIMULATIONS

EMPIRICAL MODEL SET-UP - A number of finite element calculations have been simulated using the MADYMO 2D airbag model [13,14]. In this model the airbag is represented by an ellipsoid. The spatial bag dimensions are used for calculation of penetration volumes and contact forces. The contact force can be divided in a pressure component and a tension component. The pressure component follows from the product of the actual contact area and the internal overpressure. To account for tension forces in the bag fabric is not obvious. In order to estimate the tension component some empirical airbag models, among which the MADYMO 2D and CAL-3D models, use an effective contact area. The tension component in these models is equal to the internal overpressure multiplied by the difference of effective contact area and actual contact area. From the finite element simulations an effective contact area was found identical to the area shown in Figure 15. This is illustrated on the basis of simulation results of the sphere 165 mm impactor for variation b. Figure 16 shows the calculated effective area, the quotient of contact force and bag overpressure, as a function of time. In this figure the ranges of effective areas obtained from the simulated kinematics, in accordance with Figure 15, are also shown. An excellent correlation can be observed.

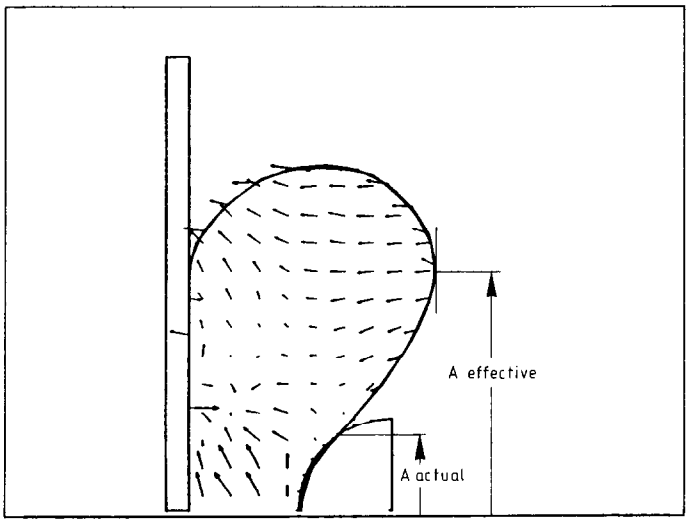

Fig. 15 Definition of actual and effective contact areas

During the first 15 ms of the MADYMO simulation the bag is filled up to 4000 N/m^2 overpressure. At 20 ms the impactor face, having an initial velocity, starts penetrating the airbag. The support plane in MADYMO

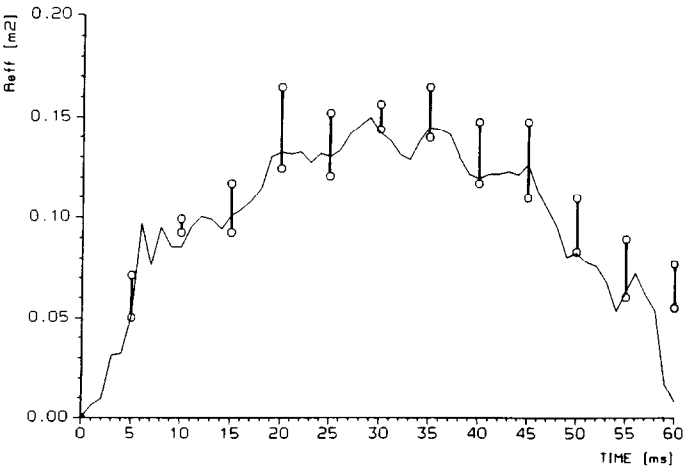

Fig. 16 Comparison between the calculated effective area and this area obtained from the contour plots

can penetrate the airbag from behind. The impactor faces are represented by elliptical cylinders in the model. For the spherical impactors an ellipse is used in the plane of simulation with a radius identical to the radius of the actual impactor. For the circular plate impactors a flat ellipse in the plane of simulation is used with a length identical to the diameter of the actual impactor and a 2 mm thickness. The width perpendicular to the plane of simulation is taken identical to the actual maximum impactor width, except for the sphere 500 mm impactor where the width is taken 2/3 of the actual diameter of the sphere. An asterisk (*) in Table 5 indicates the impact configurations simulated with the MADYMO 2D airbag model. As with the finite element simulations, the MADYMO simulations have been conducted for a low and a high impact velocity. Initially, bag elasticity will not be taken into account in the MADYMO simulations. The simulation results will be compared with the corresponding PISCES results, obtained with a normal bag stiffness (variations a and b in Table 5).

RESULTS - Since the results of the circular plate impactor with a diameter of 500 mm appeared to be close to the results of the infinite plate impactor, only the results for the latter impactor will be presented here. For the same reason the results of the very small circular plate impactor (diameter 80 mm) will be omitted here, since they showed similar tendencies as the results of the small spherical impactor (diameter 165 mm). The simulated kinematics after 30 ms for the four resulting impactor shapes are shown in Figure 17.

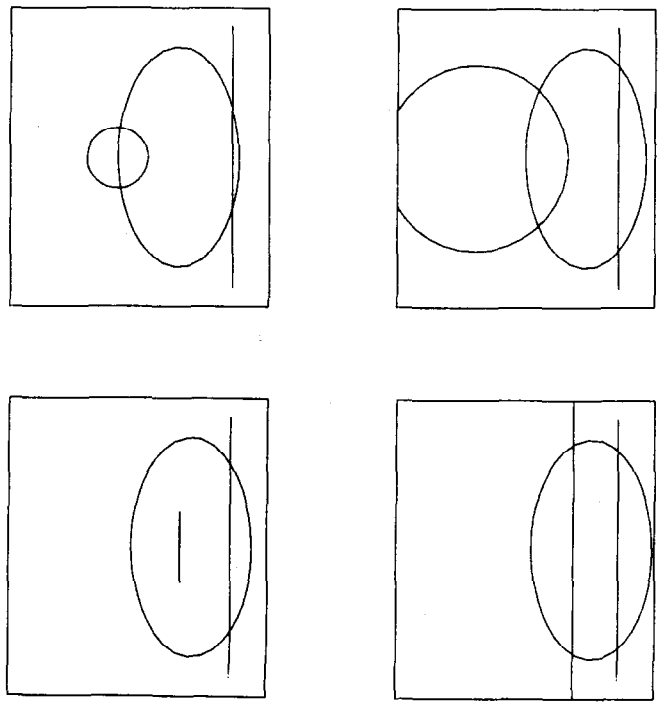

Fig. 17 Simulated kinematics after 30 ms for four different impactor shapes

For the fact that during a MADYMO simulation a direct relation between bag volume and internal bag pressure exists, for a sealed bag, the calculated pressures are not presented here. In Figure 18 the calculated bag volumes by PISCES and MADYMO are compared for the different impactor shapes. The PISCES results for the low and high velocity simulations are denoted by "var.a" and "var.b", respectively. The MADYMO results for these simulations are denoted by "madymo a" and "madymo b", respectively.

For the small penetrating object (sphere 165 mm) the decrease of bag volume is underestimated in MADYMO and consequently a larger penetration in the bag can be observed. For the circular plate 200 mm impactor the bag volume decrease and maximum bag penetration are predicted correctly. For the larger impact surfaces the prediction of the bag volume decrease is slightly too high and consequently the penetration in the bag is slightly too low. In other words, for small impactor shapes the pressure predicted by MADYMO for a certain penetration is too small, for medium sized impactor shapes the pressure prediction is correct and for larger penetrating objects the pressure is slightly overpredicted.

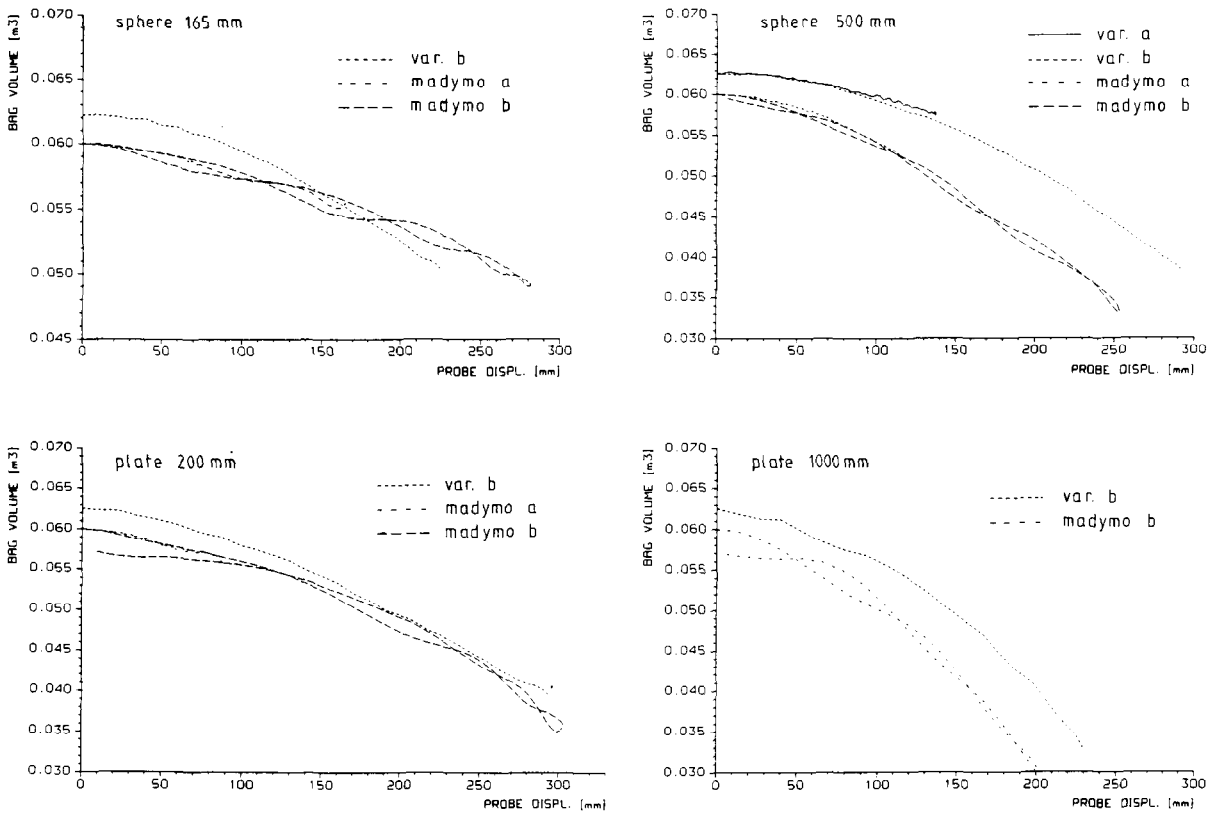

Fig. 18 Comparison of bag volumes calculated by PISCES and MADYMO for different impactor shapes

The resulting contact force in MADYMO is found from multiplying the internal bag overpressure by an effective contact area. Note that the calculated contact force can be correct, if the bag volume is underestimated and the effective contact area is overestimated, or the other way around. In Figure 19 the calculated contact forces by PISCES and MADYMO are compared for the different impactor shapes. It can be seen that for the small penetrating object (sphere 165 mm) the contact force is too small, due to underestimation of both the bag pressure and the effective contact area. The contact force calculation is correct for the circular plate 200 mm impactor. However, for large penetrating objects (sphere 500 mm and infinite plate), the contact forces are slightly too large due to overestimation of the bag pressure. This overestimation can be reduced by the introduction of bag material elasticity.

In order to evaluate the influence of bag elasticity on the MADYMO results, the simulations were repeated with a bag stretch factor. A linear dependency between bag volume V_b and internal bag overpressure ($P - P_a$) is assumed in the MADYMO 2D airbag model:

$$(V_b - V_f) / V_f = S (P - P_a) \qquad (1)$$

where S is the bag stretch factor, a material property, and V_f is the final bag volume under atmospheric conditions. According to the above equation, the bag stretch factor follows from the relation between bag volume and internal bag overpressure. This relation can de derived experimentally or from a finite element simulation. Here, a bag stretch factor of 2.E-6 m^2/N was estimated, corresponding with a volume increase of 20 % for one atmosphere overpressure.

With the introduction of bag stretch the initial bag volume in MADYMO (for 4000 N/m^2 overpressure) has increased 0.5 liters. In the PISCES simulations the initial volume is about 2 liters larger. Probably the initial bag volume in the finite element model is slightly larger due to the use of uniaxial tensile tests for determination of the bag fabric properties. It was found that the inclusion of bag stretch in the MADYMO 2D airbag model reduces the bag volume decrease considerably during penetration. The bag gets less stiff, resulting in an overall reduction of the calculated contact force. Although this improves the simulation results for large penetrating objects, the results for small penetrating objects become slightly worse, as expected. In Figure 20 the MADYMO contact force predictions obtained with stretch are presented together with the PISCES results.

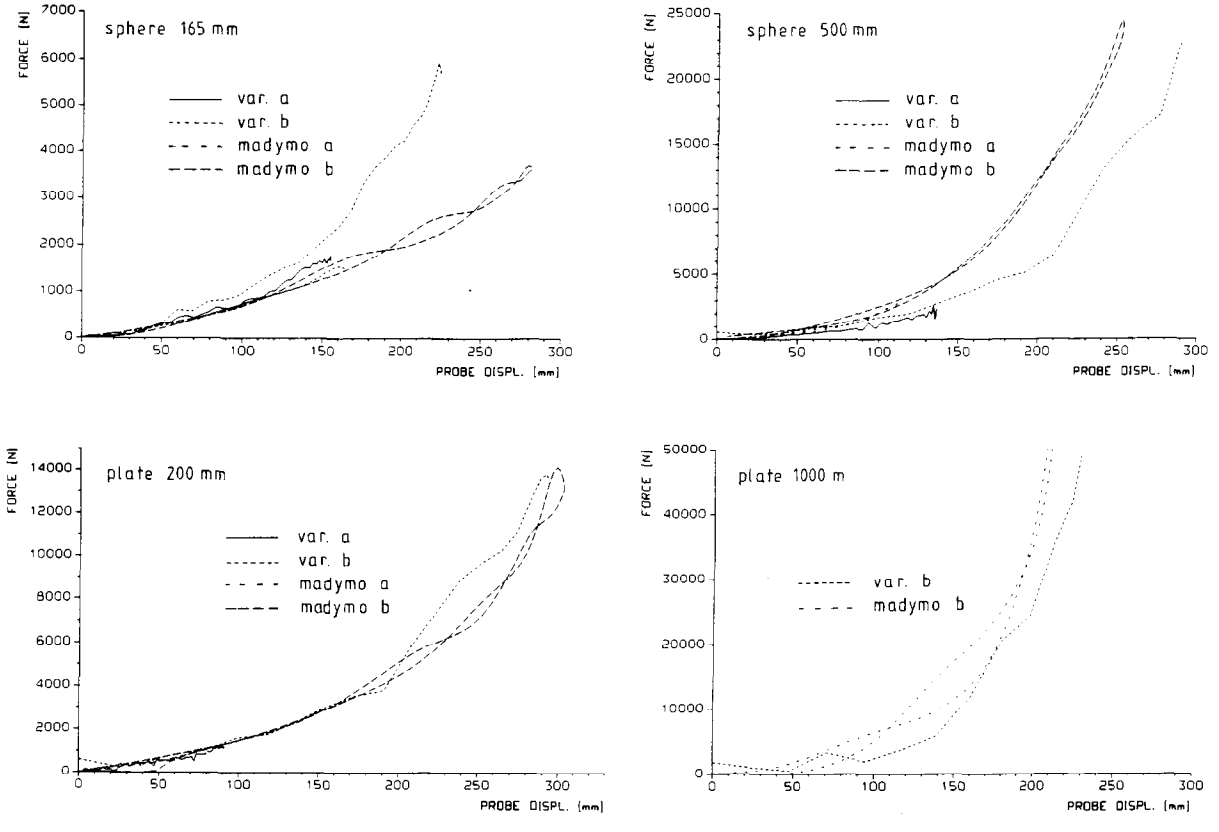

Fig. 19 Comparison of contact forces calculated by PISCES and MADYMO for different impactor shapes

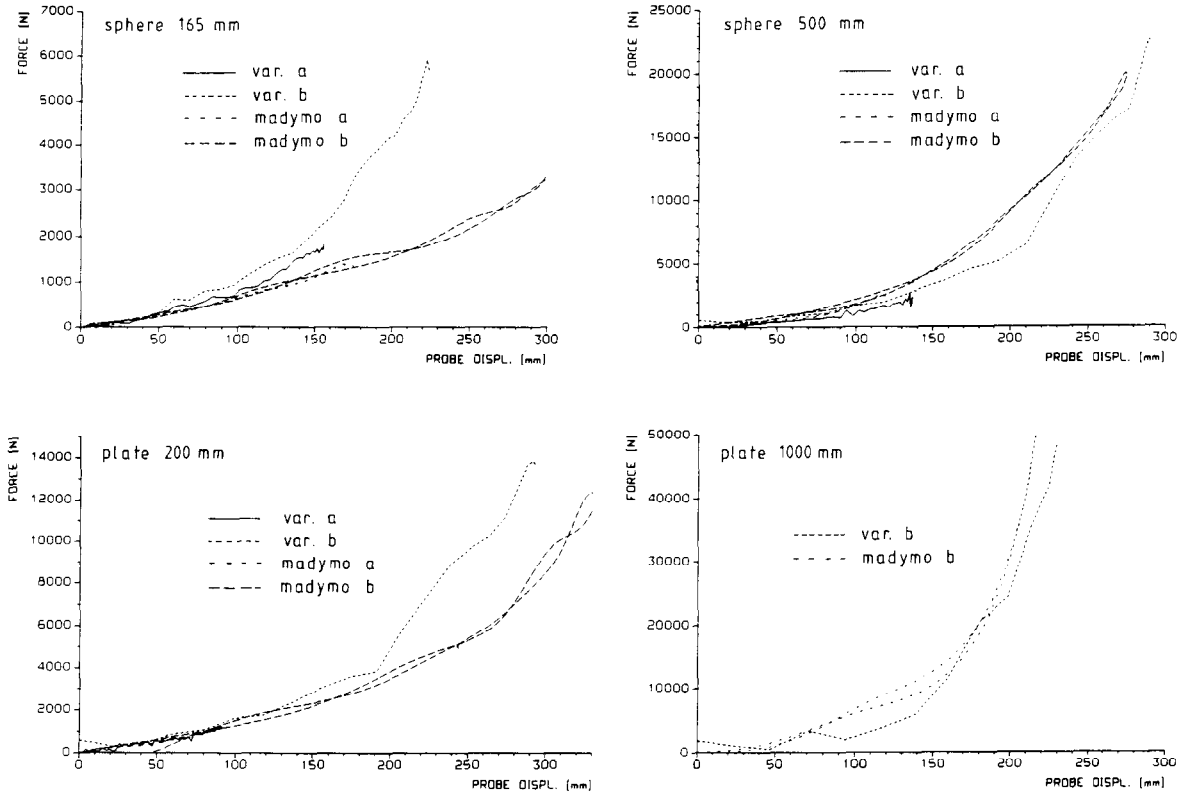

Fig. 20 Comparison of contact forces calculated by PISCES and MADYMO (with stretch) for different impactor shapes

THE MADYMO 3D AIRBAG MODEL

Although the current empirical models have proved to be valuable tools in the design process of airbag systems, these models have their limitations. To overcome these limitations, future developments in the field of airbag modelling are expected to focus more and more on the application of finite elements. A finite element approach offers for instance realistic airbag deformations and the possibility of simulating out-of-position occupants. Disadvantages of the currently available finite element airbag models, however, are the model complexity and the relatively long computer run times required. Moreover, practical use of these models for occupant protection studies depends on a coupling with a CVS program, since finite element programs do not provide features like various belt systems and realistic and efficient occupant models. A step forward is the development of a relatively simple finite element airbag model as an integral part of a CVS program.

Such a model recently has been developed for the MADYMO 3D CVS program. This model utilizes 3-node membrane elements with linear elastic isotropic material properties and the central difference method for time integration. The model is optimized for airbag simulation in a CVS environment. For example, the airbag can be connected directly to any element of any system in MADYMO and a special contact logic is included for the definition of contact between airbag nodes and ellipsoids. Together with the application of relatively simple gas dynamics, compared to an Euler gasflow discretization, acceptable computer run times are achieved. Figure 21 shows a first demonstration of the MADYMO 3D airbag model. The airbag is mounted to a flat ellipsoid support and is impacted by a rigid sphere, having a mass of 10 kg and an initial velocity of 10 m/s. Gravitation acts only on the sphere. Table 6 specifies the computer run time required on a Silicon Graphics 4D/20G workstation for 120 ms of simulation, using various numbers of elements. A mesh of about 1000 elements is considered to be sufficient for a driver side airbag simulation. Further savings in computer run time can be accomplished by mesh differentiation and a more selective contact specification. It is planned to include straps, linear elastic orthotropic material properties, contact friction and wrinkling elements in the first version of the MADYMO 3D airbag model. Wrinkling ele-

ments account for tension only in the bag fabric. The wrinkling option allows the airbag to be modelled with a relatively coarse mesh.

Table 6 Computer time required for the colliding ball example

number of elements	CPU-min.
128	3
432	13
1024	46
3456	300

DISCUSSION AND CONCLUSIONS

In this study an engineering analysis has been carried out on the interaction between a driver side airbag and a rigid body. Computer simulations as well as component tests for validation purposes have been conducted. In the component tests sealed airbags were penetrated in the center by different impactor faces at various impact velocities. From these tests a considerable influence of the impactor shape and size could be observed. The effect of the support (i.e. flat support versus steering wheel rim) was found to be very small.

The component tests have been simulated with the PISCES 2D-ELK code, where for representation of the gas inside the airbag an Euler discretization was used. In general, very realistic simulations of the airbag response could be observed, offering a detailed insight into the bag shape changes. Using this validated model set-up, a parametric study was conducted where the impact velocity, the bag material elasticity and the bag support shape were varied. The larger impact velocities resulted in much higher penetrations of the impactor in the airbag. As a result much larger deformations of the bag contour could be observed. The increased impact velocity, however, did not influence the resistive force experienced by the impactor face. In other words, for the selected range of impact velocities (up to 24 m/s) inertia effects of the bag material can be neglected. However, note that in case of a deploying airbag higher relative impact velocities can be expected. As in the component tests the effect of a steering wheel support instead of a flat plate support appears to be small. So for many applications it is probably not needed to describe in detail the geometry of the steering wheel rim. Considerable effects of bag material elasticity could be observed, especially on the bag volume.

Another finding concerns the bag tension forces. In some empirical airbag models an effective area is used to estimate the contribution of the tension forces. The tension force in these models is equal to the internal bag overpressure multiplied by the difference of effective contact area and actual contact area. The finite element simulations presented show that the effective contact area can be determined directly from the deformed airbag shape. The contribution of the tension forces is larger for small impacting surfaces. For large impact surfaces this contribution is much smaller or even absent in the case of an infinite surface.

The empirical airbag model in MADYMO 2D was used to simulate a number of finite element calculations. It was found that the contact algorithms in this model are working adequately for penetration of average and large sized objects. There is a good agreement with the FEM simulation results. For large sized objects the contact forces are slightly overestimated. This overestimation can be reduced by the introduction of bag material elasticity in the MADYMO 2D airbag model. In general this introduction will positively influence driver airbag simulations. The model predictions for small penetrating objects are less adequate. This will affect in particular passenger side airbag simulations. For example, the head of an occupant is relatively small compared to the dimensions of a passenger side bag. Due to the two-dimensional nature of the MADYMO model the impactor shapes are not simulated fully correct, compared to the three-dimensional axi-symmetric representation in the PISCES 2D-ELK code. Some simulation results might be slightly affected by this.

It should be noted that the findings obtained here are based on axi-symmetric tests on a sealed airbag using several sizes of rigid impactors. Therefore the results of this study should not be interpreted to represent general airbag contact interactions. The pressure build-up inside an airbag in action is different for example, mainly due to gas exhaust from the bag. Moreover, impactor face deformation due to airbag contact has not been taken into account for this study. Although of minor importance compared to airbag deformation, this phenomenon could be studied by using finite elements for representation of the impacting body as well.

As mentioned earlier, future developments in the field of airbag modelling will be focussed more and more on the application of finite elements in order to overcome the limitations of empirical airbag models. The finite element MADYMO 3D airbag model was introduced as an addition to the existing finite element airbag models in PAM-CRASH, PISCES and DYNA 3D. For occupant protection studies the latter models are committed to a coupling with a CVS program. The MADYMO 3D airbag model uses relatively simple gas dynamics and linear elastic material properties, whereas the other finite element airbag models apply

more detailed material models and/or an Euler discretization for the gasflow inside the airbag (PISCES). Although the computer run times required for the coupled finite element models are longer, more information can be obtained from these models. In future more effort should be put into the simulation of realistic airbag deployment. For this purpose complicated mesh folding mechanisms have to be developed.

It is believed that computer simulation of the airbag response is an important research activity. Well validated and highly reliable airbag models can provide a valuable contribution to the design of optimal airbag systems. Occupants involved in automobile crashes would directly benefit from this effort.

ACKNOWLEDGEMENTS

The authors wish to acknowledge the Motor Vehicle Manufacturers Association of the United States Inc. for funding part of this study. The opinions, findings and conclusions expressed in this publication are those of the authors and not necessarily those of the MVMA Inc. or its members. The authors also wish to acknowledge the MacNeil-Schwendler Company B.V. (formerly PISCES International B.V.) for performing the PISCES finite element airbag simulations.

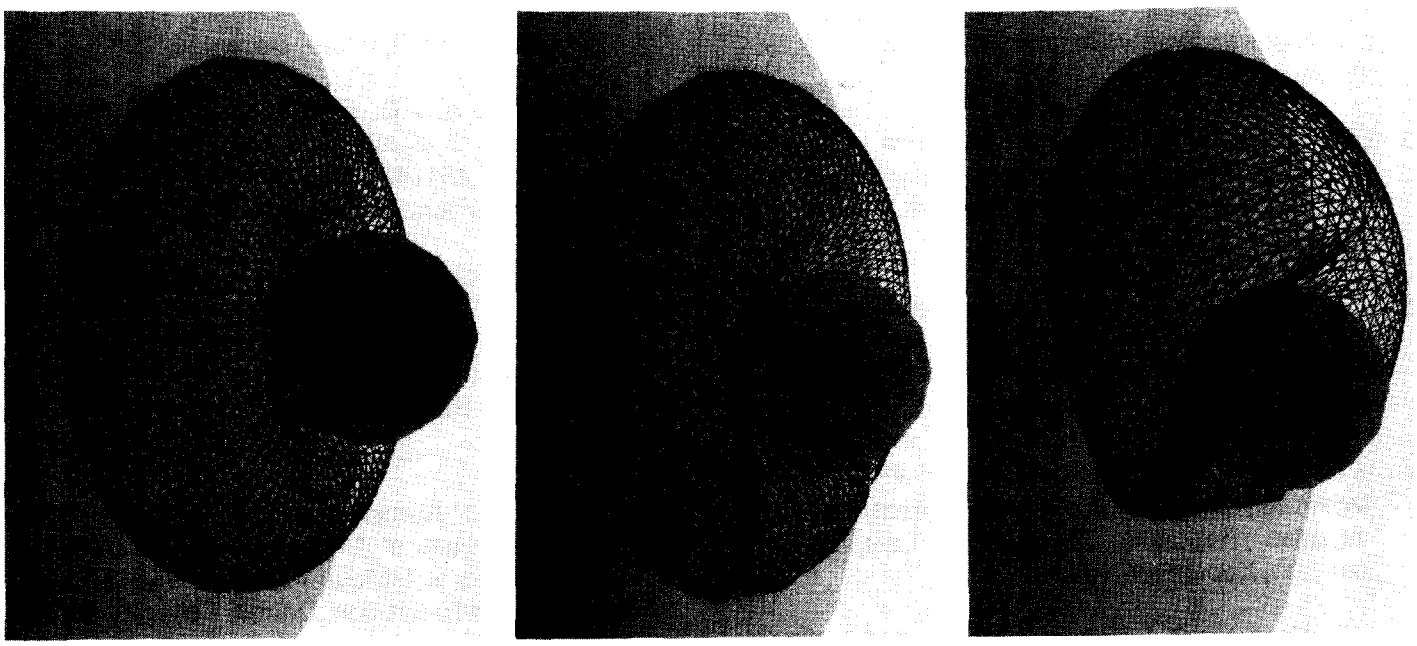

Fig. 21 Colliding ball simulation using the MADYMO 3D airbag model (3456 elements)

REFERENCES

1. M.V. Fitzpatrick - Development of a Driver Air Cushion (DRAC) Computerized Math Model of an Ellipsoidal Airbag Reacting in Two Dimensions on a Production Type Steering Assembly ; 8th International Conference on Experimental Safety Vehicles, Wolfsburg, October 21-24, 1980.

2. "BDRACR" User's Manual, Version 5.14 ; Fitzpatrick Engineering, June 10, 1985.

3. "BPAC" User's Manual, Version 3.36 ; Fitzpatrick Engineering, June 10, 1985.

4. B.M. Bowman, R.O. Bennett and D.H. Robbins - MVMA Two-Dimensional Crash Victim Simulation, Version 4, Volume 1 ; Final Report UM-HSRI-79-5-1, Highway Safety Research Institute, June 29, 1979.

5. C.C. Chou, A. Lev and D.M. Lenardon - MVMA-2D Air Bag/Steering Assembly Simulation Model ; SAE 800298, Congress and Exposition, Detroit, February, 1980.

6. J.J. Nieboer, J. Wismans and E. Fraterman - Status of the MADYMO 2D Airbag Model ; SAE 881729, 32nd Stapp Car Crash Conference, Atlanta, October 17-19, 1988.

7. J.T. Fleck and F.E. Butler - Validation of the Crash Victim Simulator, Volume 1, Part 1: Analytical Formulation ; Report No. ZS-5881-V-1, Calspan Corporation, December, 1981.

8. J.T. Wang and D.J. Nefske - A New CAL3D Airbag Inflation Model ; SAE 880654, Congress and Exposition, Detroit, February 29-March 4, 1988.

9. R. Hoffman, A.K. Pickett, D. Ulrich, E. Haug, D. Lasry and J. Clinkemaillie - A Finite Element Approach to Occupant Simulation: The PAM-CRASH Airbag Model ; SAE 890754, International Congress and Exposition, Detroit, February 27-March 3, 1989.

10. R. Hoffman and D. Lasry - Design for Passive Safety using Numerical Simulation Techniques ; 50th Anniversary Symposium, Wayne State University, Detroit, November 10, 1989.

11. W.E.M. Bruijs, A.J. Buijk, P.J.A. de Coo and A.A.H.J. Sauren - Validation of Coupled Calculations with MADYMO and PISCES Airbag ; Proceedings of the 2nd International MADYMO User's Meeting, Noordwijk, May 14-15, 1990.

12. A.M.A. van der Heijden, A.J. Buijk and P.H.L. Groenenboom - Numerical Simulation of Airbag Behaviour ; Proceedings Susi Conference, Cambridge, July 11-13, 1989.

13. MADYMO User's Manual 2D, Version 4.2 ; TNO Road-Vehicles Research Institute, October 1988.

14. P.J.A. de Coo, J.J. Nieboer and J. Wismans - Computer Simulation of Driver Airbag Contact with Rigid Body ; Report No. 751960020 / MVMA Agreement No. TNO 8909-C9137, TNO Road-Vehicles Research Institute, December 1989.

15. R. Brandman and D. Breed - Use of Computer Simulation in Evaluating Airbag System Performance ; SAE 851188, Government/Industry Meeting and Exposition, Washington, May 20-23, 1985.

16. M.V. Fitzpatrick and D.J. Biss - Development of the DEPLOY Computerized Math Model of the Interaction of an Occupant's Chest with a Deploying Air Bag ; Eight International Conference on Experimental Safety Vehicles, Wolfsburg, October 21-24, 1980.

17. D.J. Biss, D.J. Romeo and B.S. Peterson - The Biokinetical Limits of Air Bag Protection of Small Car Occupants in Oblique Impacts ; SAE 870330, Congress and Exposition, Detroit, February 23-27, 1987.

18. S. Enouen, D.A. Guenther, R.A. Saul and T.F. MacLaughlin - Comparison of Models Simulating Occupant Response with Air Bags ; SAE 840451, Congress and Exposition, Detroit, February 27-March 2, 1984.

19. A.I. King, C.C. Chou and J.A. MacKinder - Mathematical Model of an Airbag for Three-Dimensional Occupant Simulation ; SAE 720036, Automotive Engineering Congress, Detroit, January 10-14, 1972.